Electronic Supporting Information

A First-Principles Prediction on "Healing Effect" of Graphene Preventing Carrier Trapping near the Surface of Metal Halide Perovskites

Wei-Wei Wang,[1,2] Jing-Shuang Dang,[1,2] Ryota Jono,[1] Hiroshi Segawa,*[1] and Manabu Sugimoto*[1,2]

1) Research Center for Advanced Science and Technology, The University of Tokyo, 4-6-1 Komaba, Meguro-ku, Tokyo 153-8904, Japan
2) Faculty of Advanced Science and Technology, Kumamoto University, 2-39-1 Kurokami, Chuo-ku, Kumamoto 860-8555, Japan

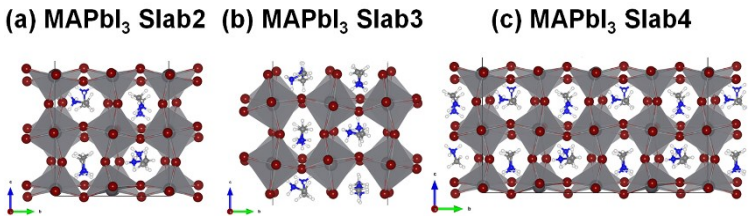

Figure S1. Other $MAPbI_3$ slabs with different sizes and terminations (side-view).

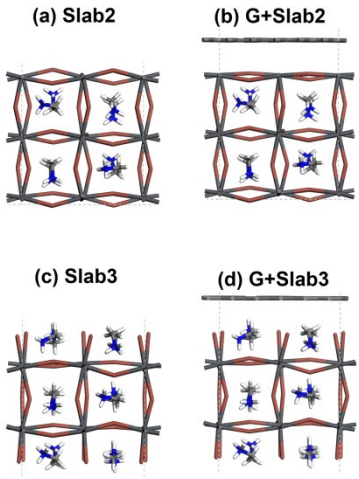

Figure S2. PbI_2-terminated (Slab2) and MAI-terminated (Slab3) $MAPbI_3$ slabs and corresponding graphene(G)+$MAPbI_3$ hybrids.

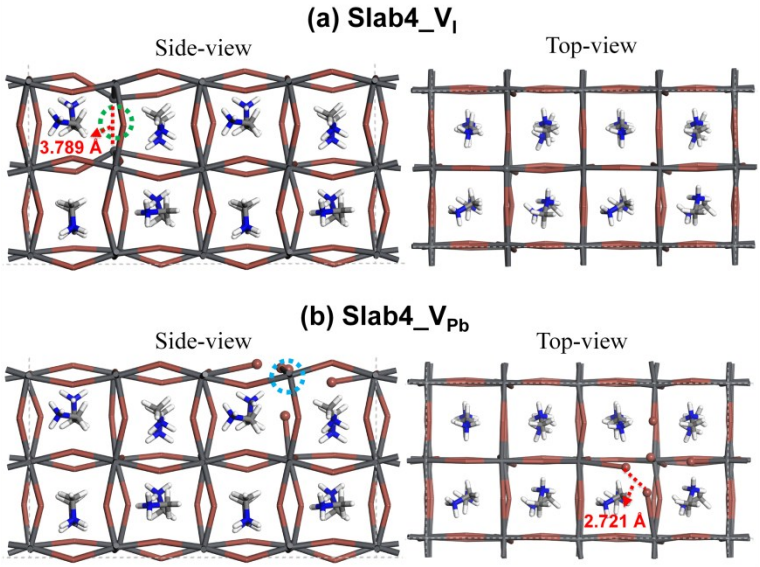

Figure S3. Defective $MAPbI_3$ slabs (Slab4) with: (a) I vacancy and (b) Pb vacancy.

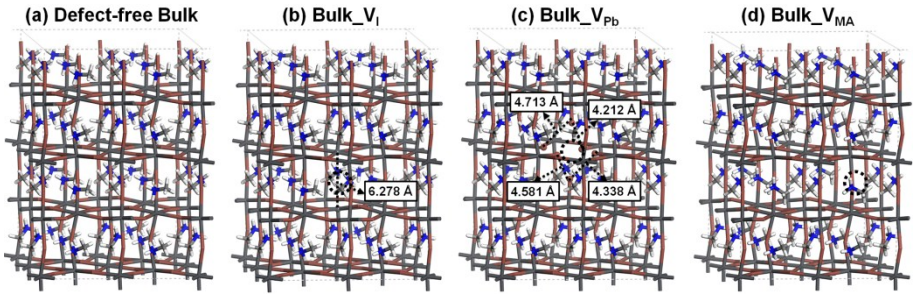

Figure S4. The optimized structures of (a) defect-free, (b) V_I-containing, (c) V_{Pb}-containing, and (d) V_{MA}-containing bulk $MAPbI_3$ structures. The positions of the single vacancies are depicted by the dashed circles.

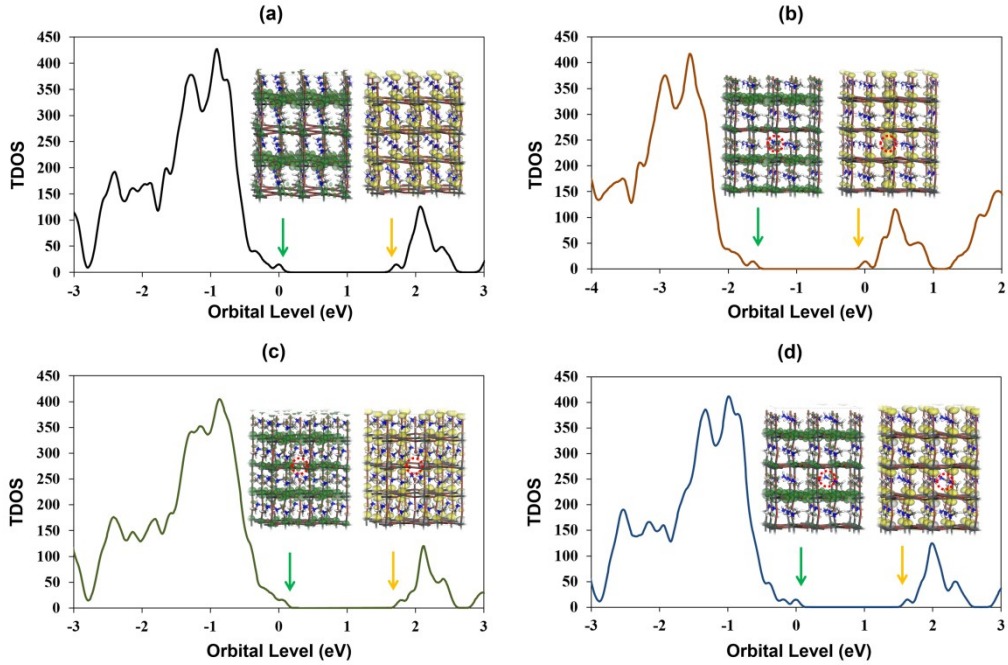

Figure S5. Calculated total density of states (TDOS) of (a) defect-free (b) V_I-containing, (c) V_{Pb}-containing, and (d) V_{MA}-containing bulk $MAPbI_3$ structures. The insets show the orbital shape of the band edges (isovalue: 0.002 a.u.). The Fermi level is set to zero.

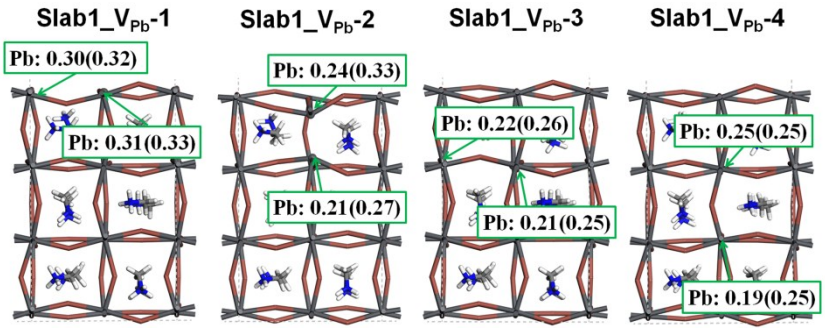

Figure S6. Hirshfeld charge (e) of dangling Pb atoms in V_I-containing Slab1. A value in a parenthesis indicates the charge in defect-free Slab1.

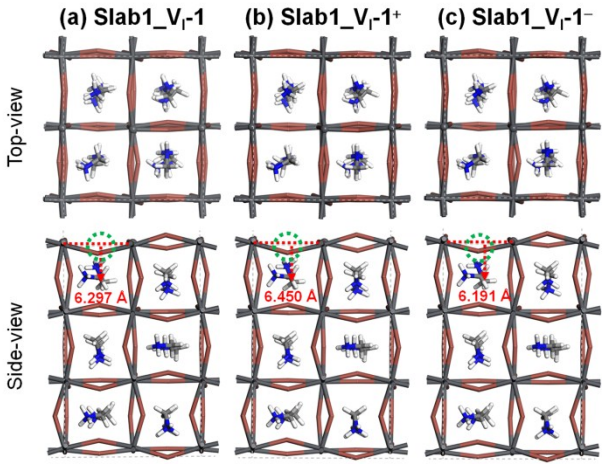

Figure S7. Neutral and charged $MAPbI_3$ slabs with V_I (Slab1_V_I-1): (a) Slab1_V_I-1, (b) Slab1_V_I-1$^+$, and (c) Slab1_V_I-1$^-$.

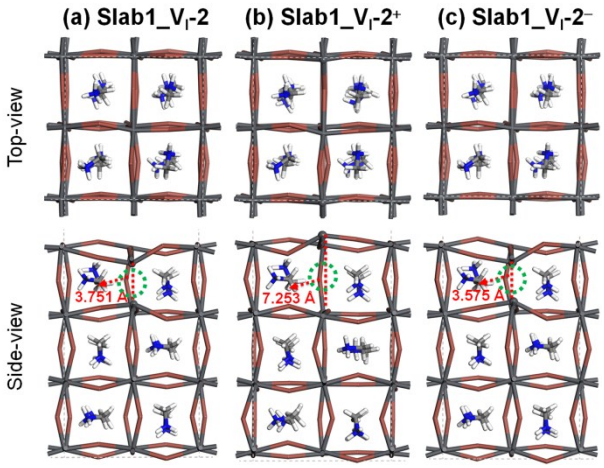

Figure S8. Neutral and charged $MAPbI_3$ slabs with V_I (Slab1_V_I-2): (a) Slab1_V_I-2, (b) Slab1_V_I-2$^+$, and (c) Slab1_V_I-2$^-$.

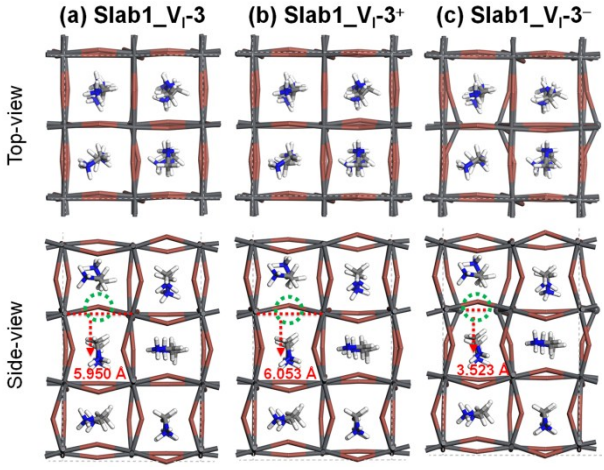

Figure S9. Neutral and charged $MAPbI_3$ slabs with V_I (Slab1_V_I-3): (a) Slab1_V_I-3, (b) Slab1_V_I-3$^+$, and (c) Slab1_V_I-3$^-$.

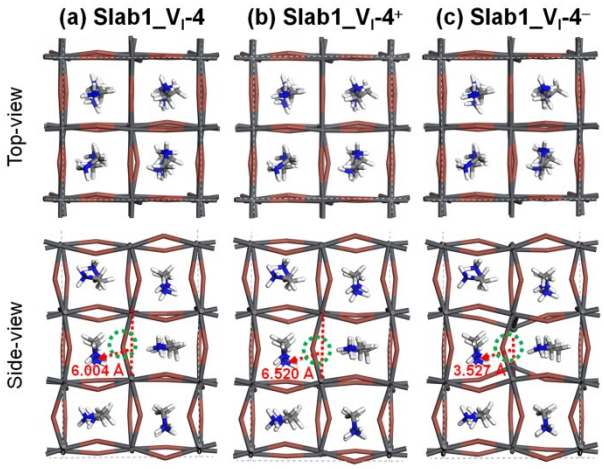

Figure S10. Neutral and charged $MAPbI_3$ slabs with V_I (Slab1_V_I-4): (a) Slab1_V_I-4, (b) Slab1_V_I-4$^+$, and (c) Slab1_V_I-4$^-$.

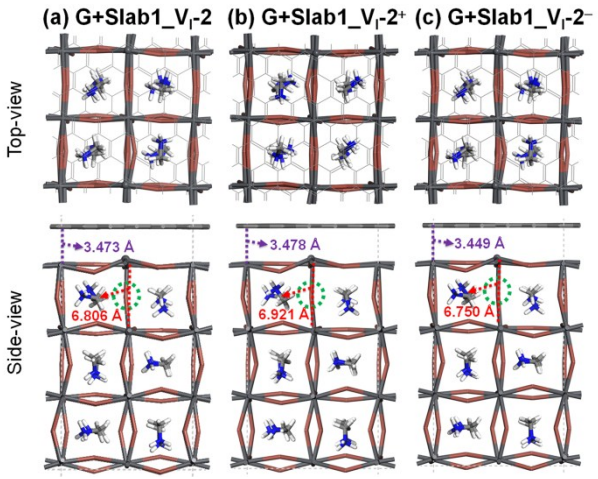

Figure S11. Neutral and charged G+Slab1_V_I-2: (a) G+Slab1_V_I-2, (b) G+Slab1_V_I-2$^+$, and (c) G+Slab1_V_I-2$^-$.

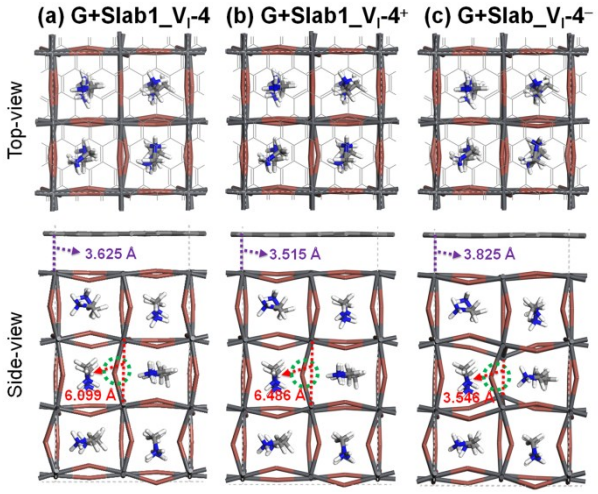

Figure S12. Neutral and charged G+Slab1_V_I-4: (a) G+Slab1_V_I-4, (b) G+Slab1_V_I-4$^+$, and (c) G+Slab1_V_I-4$^-$.

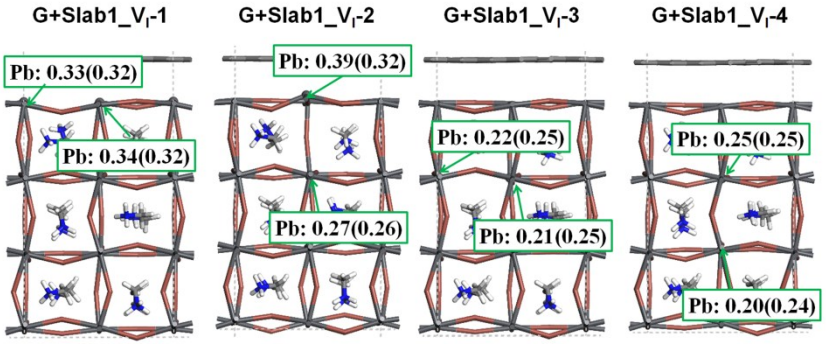

Figure S13. Hirshfeld charge (e) of dangling Pb atoms in V_I-containing G+Slab1. A value in a parenthesis indicates the charge in defect-free G+Slab1.

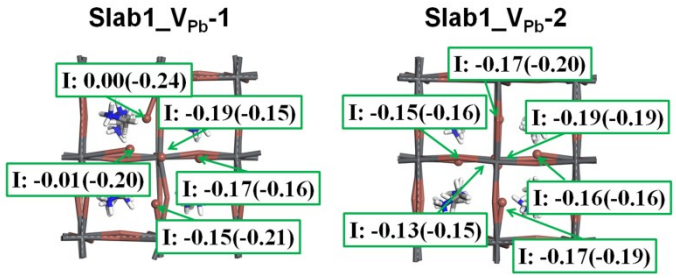

Figure S14. Hirshfeld charge (e) of dangling I atoms in V_{Pb}-containing Slab1. A value in a parenthesis indicates the charge in defect-free Slab1

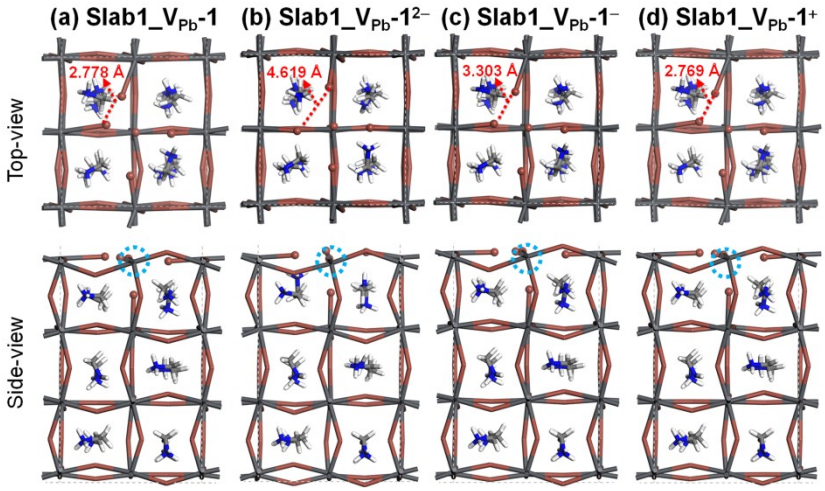

Figure S15. Neutral and charged defective $MAPbI_3$ slabs with V_{Pb} (Slab1_V_{Pb}-1): (a) Slab1_V_{Pb}-1, (b) Slab1_V_{Pb}-1^{2-}, (c) Slab1_V_{Pb}-1^{-}, and (d) Slab1_V_{Pb}-1^{+}.

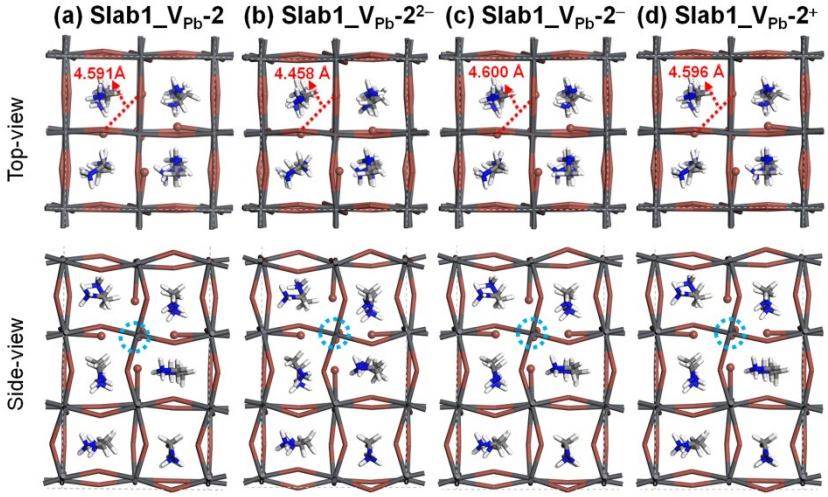

Figure S16. Neutral and charged defective $MAPbI_3$ slabs with V_{Pb} (Slab1_V_{Pb}-2): (a) Slab1_V_{Pb}-2, (b) Slab1_V_{Pb}-2^{2-}, (c) Slab1_V_{Pb}-2^{-}, (d) Slab1_V_{Pb}-2^{+}

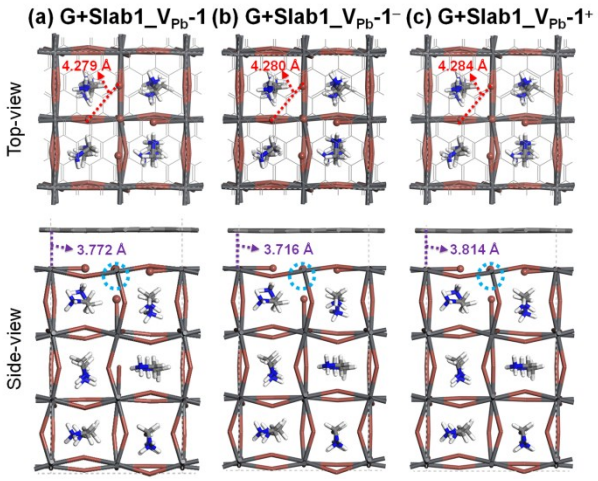

Figure S17. Neutral and charged G+Slab1_V_{Pb}-1: (a) G+Slab1_V_{Pb}-1, (b) G+Slab1_V_{Pb}-1^{-}, and (c) G+Slab1_V_{Pb}-1^{+}

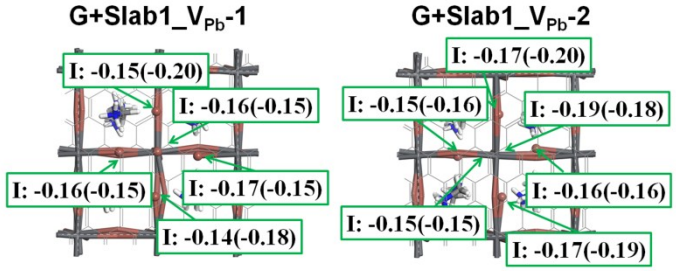

Figure S18. Hirshfeld charge (e) of dangling I atoms in V_{Pb}-containing Slab1. A value in a parenthesis indicates the charge in defect-free G+Slab1.

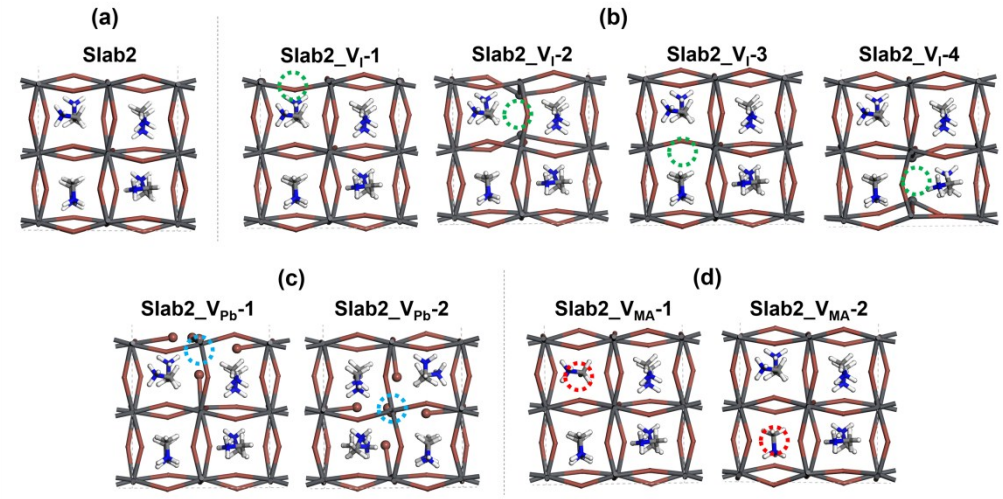

Figure S19. Optimized (a) defect-free (b) V_I-containing, (c) V_{Pb}-containing, and (d) V_{MA}-containing Slab2 structures.

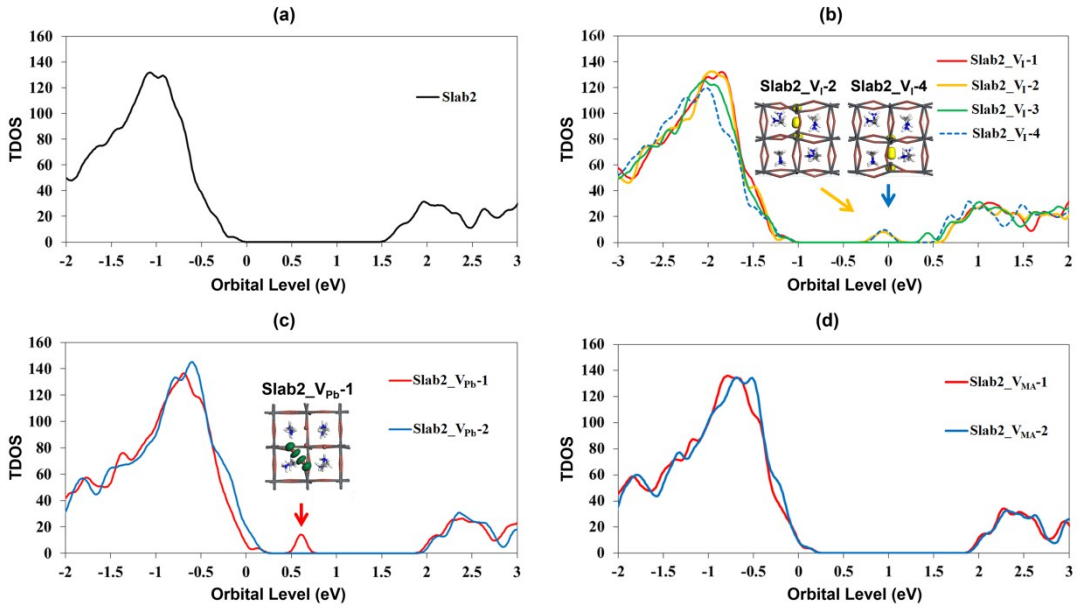

Figure S20. Calculated total density of states (TDOS) of (a) defect-free (b) V_I-containing, (c) V_{Pb}-containing, and (d) V_{MA}-containing Slab2 structures. The insets in (b) and (c) show to the orbital shape of the deep-level defects (isovalue: 0.020 a.u.). The valence band tops of all the defective slab models in (b) and (c) were adjusted to the same level.

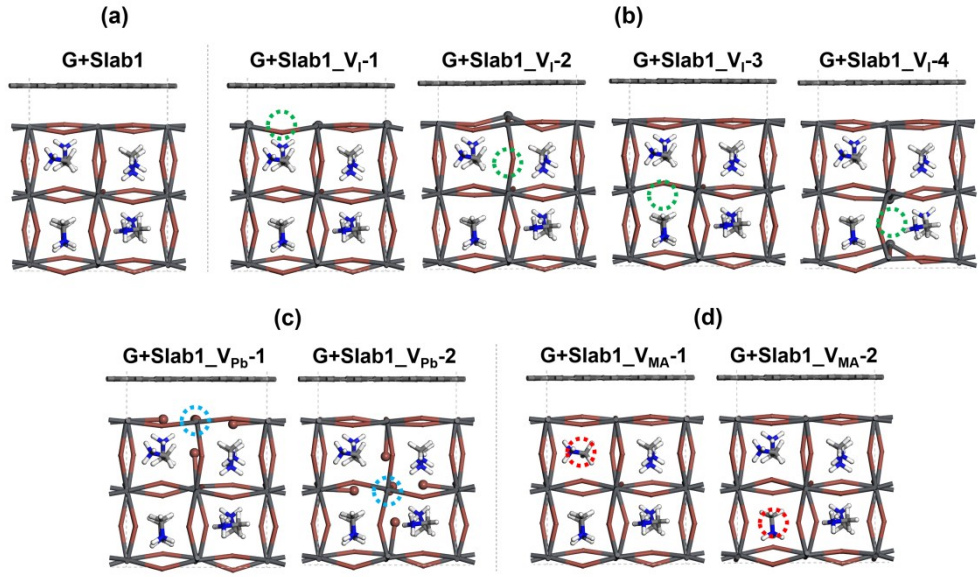

Figure S21. Optimized (a) defect-free (b) V_I-containing, (c) V_{Pb}-containing, and (d) V_{MA}-containing G+Slab2 hybrids.

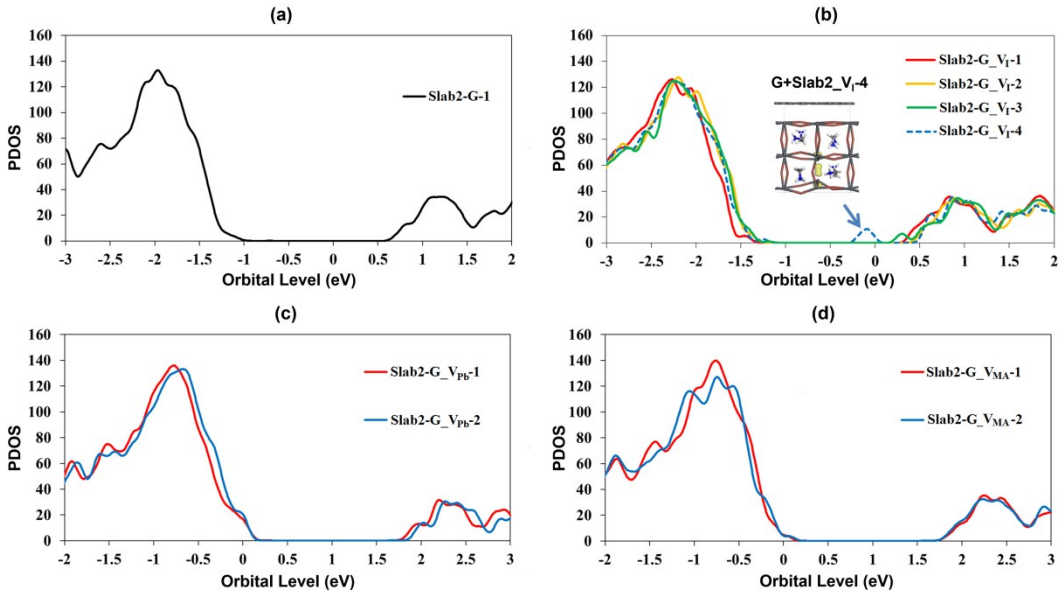

Figure S22. Calculated partial density of states (PDOS) of $MAPbI_3$ in (a) defect-free (b) V_I-containing, (c) V_{Pb}-containing, and (d) V_{MA}-containing G+Slab2 hybrids. The inset in (b) shows to the orbital shape of the deep-level defect (isovalue: 0.020 a.u.).

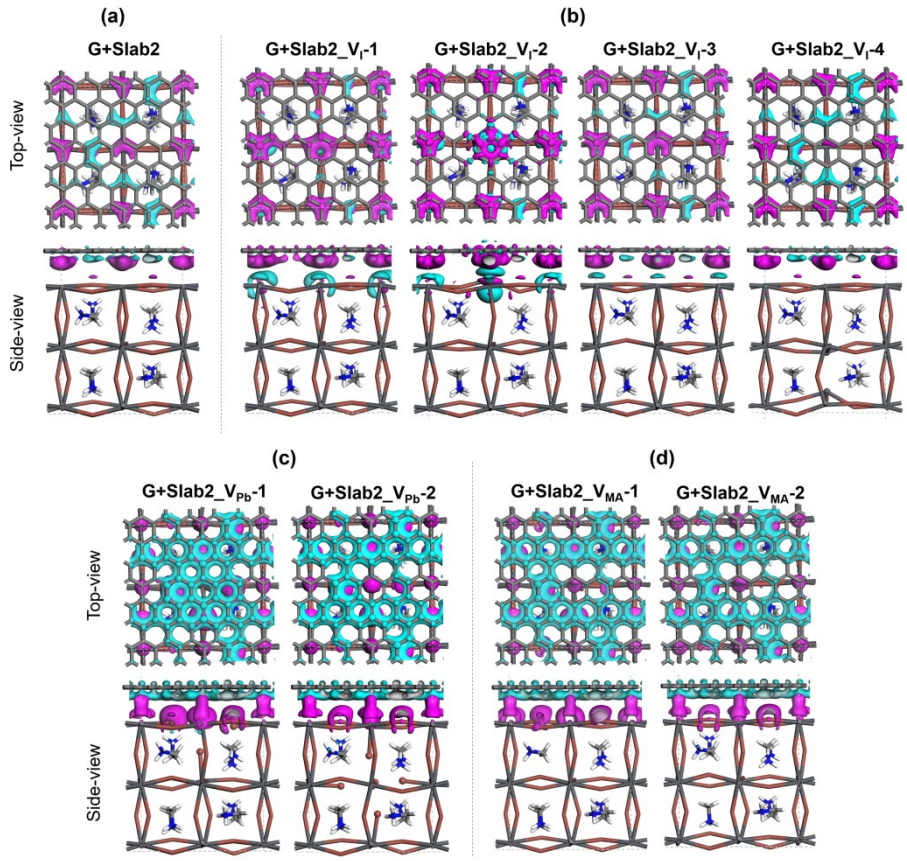

Figure S23. Electron density difference of (a) defect-free (b) V_I-containing, (c) V_{Pb}-containing, and (d) V_{MA}-containing G+Slab2 hybrids (isovalue: 0.003 a.u.). Purple and cyan represent accumulation and depletion of electrons, respectively.

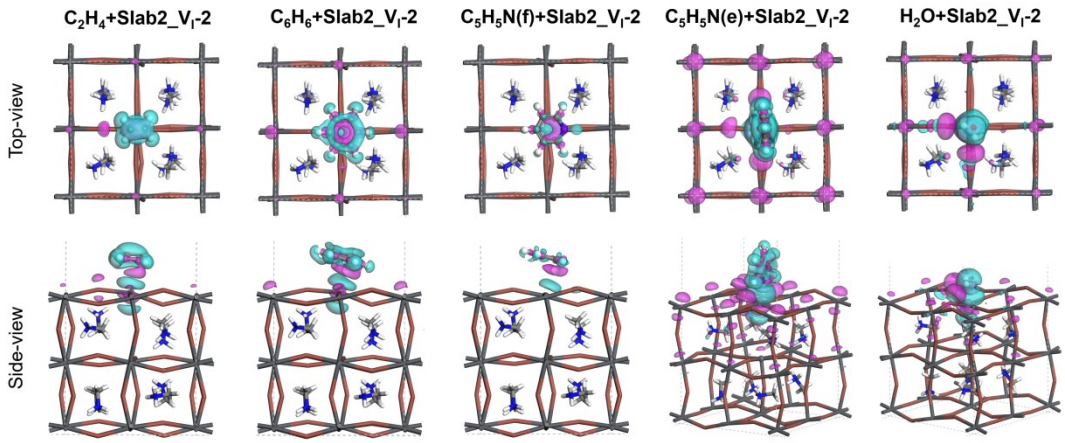

Figure S24. Electron density difference of V_I-containing molecule+Slab2_V_I-2 hybrids (isovalue: 0.003 a.u.). Purple and cyan represent accumulation and depletion of electrons, respectively.

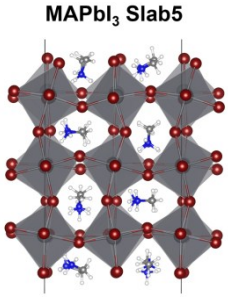

Figure S25. MAI-terminated $MAPbI_3$ slab model (Slab5).

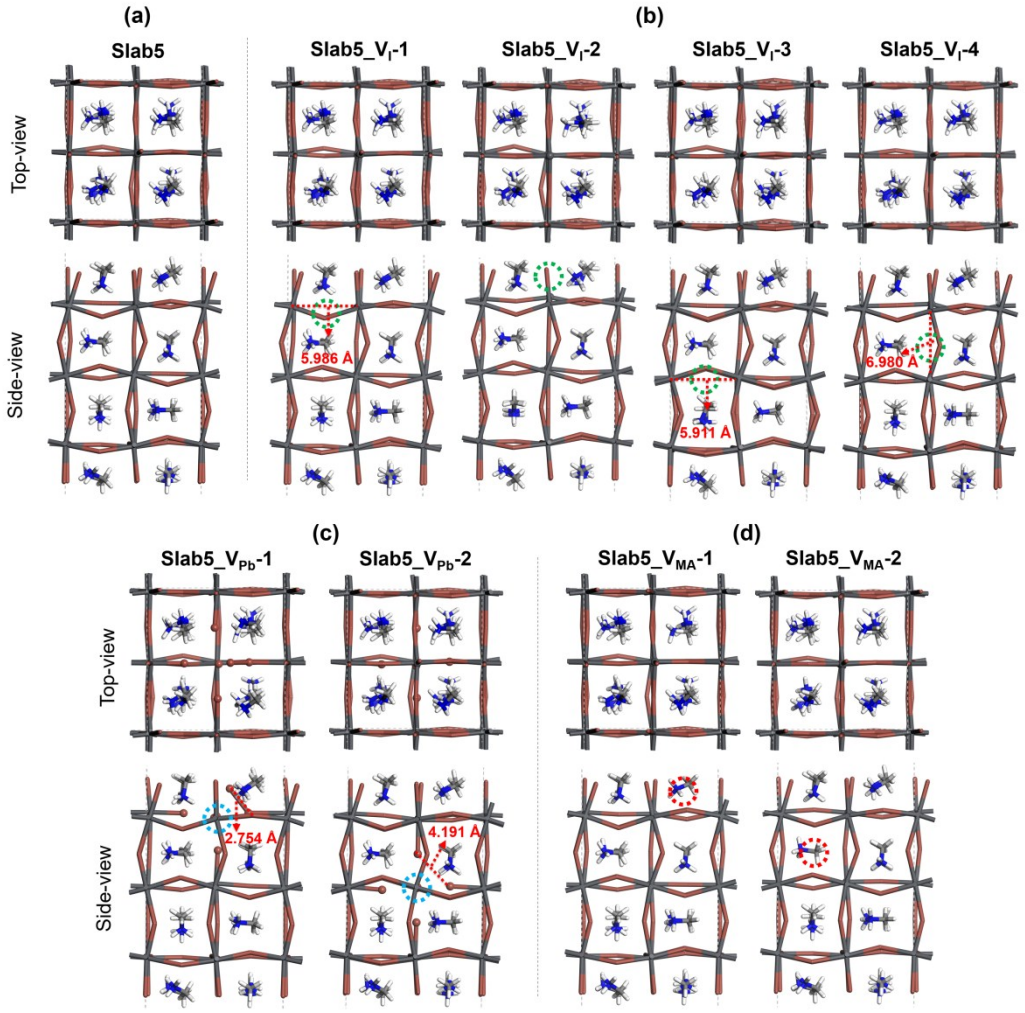

Figure S26. Optimized (a) defect-free (b) V_I-containing, (c) V_{Pb}-containing, and (d) V_{MA}-containing Slab5 structures.

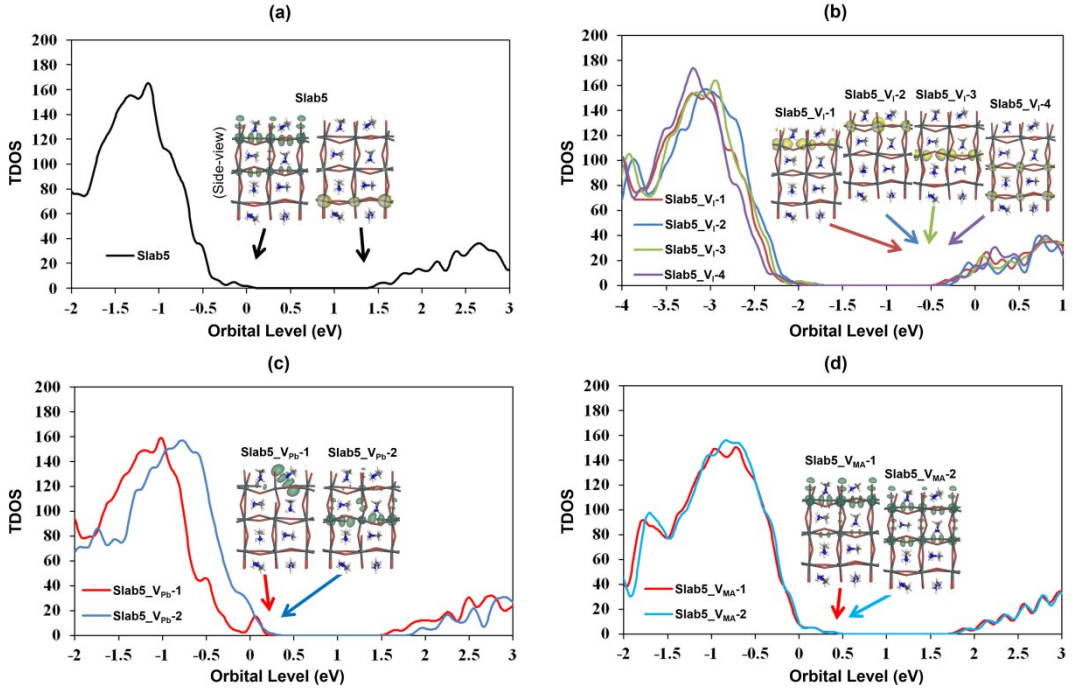

Figure S27. Calculated total density of states (TDOS) of (a) defect-free (b) V_I-containing, (c) V_{Pb}-containing, and (d) V_{MA}-containing Slab5 structures. The insets show the orbital shape of the band edges (isovalue: 0.015 a.u.).

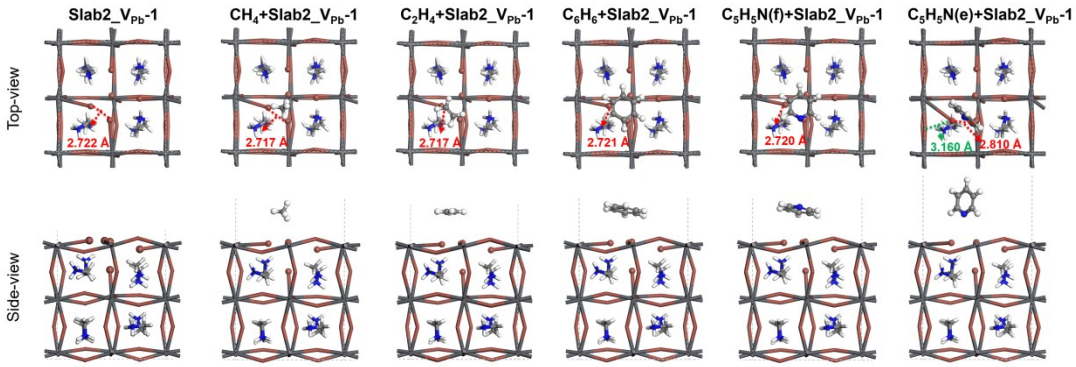

Figure S28. Structures of defective Slab2_V_{Pb}-1 and corresponding molecule+Slab2_V_{Pb}-1 hybrids.

Table S1. Calculated band gaps (E_g) of defect-free $MAPbI_3$ models [a]

$MAPbI_3$	Bulk	PbI_2-terminated slab	MAI-terminated slab
E_g (eV)	1.719	1.352	1.493

a. PbI_2-terminated and MAI-terminated $MAPbI_3$ slabs correspond to the Slab1 and Slab5, respectively.

Table S2. Binding energies (E_b) of graphene(G)+Slab2 and G+Slab3 hybrids

Hybrids	G+Slab2	G+Slab3
E_b (eV)	2.303	1.898

Table S3. Calculated binding energies (E_b) and interaction energies (E_i) of graphene(G)+Slab1 hybrids and the distortion energies (E_d) of Slab1 and graphene after hybridization [a]

Structure	E_b (eV)	E_i (eV)	E_d (eV)	
			$MAPbI_3$	Graphene
Defect-free G+Slab1	2.370	2.504	0.112	0.022
G+Slab1_V_I-1	2.319	2.446	0.110	0.017
G+Slab1_V_I-2	2.304	2.658	0.347	0.007
G+Slab1_V_I-3	2.301	2.500	0.184	0.015
G+Slab1_V_I-4	2.335	2.520	0.161	0.025
G+Slab1_V_{Pb}-1	1.626	2.684	1.043	0.015
G+Slab1_V_{Pb}-2	2.677	2.723	0.029	0.017
G+Slab1_V_{MA}-1	2.648	2.798	0.129	0.021
G+Slab1_V_{MA}-2	2.707	2.762	0.044	0.011

a. E_i (hybrid) = E'(Slab1) + E'(G) – E(hybrid), E_d(G) = E(G) – E'(G), E_d(Slab1) = E(Slab1) – E'(Slab1), where E'(Slab1) and E'(G) denote the calculated energies of distorted $MAPbI_3$ slabs and graphene after hybridization, respectively.

Table S4. Calculated binding energies (E_b) of defective graphene(G)+Slab1 hybrids (G+Slab1_V_I-2 and G+Slab1_V_{Pb}-1) and the pair formation energy (E_p) of Pb-Pb/I-I dimer in Slab1_V_I-2/Slab1_V_{Pb}-1 [a]

	E_b (eV)	E_p (eV)
Slab1_V_I-2	2.304	0.371
Slab1_V_{Pb}-1	1.626	1.221

a. The pair formation energy is defined as: E_p(Pb-Pb) = E(Slab1_V_I-2') – E(Slab1_V_I-2), E_p(I-I) = E(Slab1_V_{Pb}-1') – E(Slab1_V_{Pb}-1), where Slab1_V_I-2' and Slab1_V_{Pb}-1' denote the energies of un-optimized Slab1_V_I-2 (by removing I from optimized defect-free Slab1) and Slab1_V_{Pb}-1 (by removing Pb from optimized defect-free Slab1), respectively.

Table S5. Hirshfeld charge of graphene in G+Slab1 hybrids [a]

Structure	Hirshfeld charge of graphene (eV)
Defect-free G+Slab1	-0.20
G+Slab1_V_I-1	-0.37
G+Slab1_V_I-2	-0.34
G+Slab1_V_I-3	-0.20
G+Slab1_V_I-4	-0.23
G+Slab1_V_{Pb}-1	+0.14
G+Slab1_V_{Pb}-2	+0.07
G+Slab1_V_{MA}-1	+0.10
G+Slab1_V_{MA}-2	+0.09